Cellular/Molecular

# A Complete Genetic Analysis of Neuronal Rab3 Function

**Oliver M. Schlüter,[1,2,3] Frank Schmitz,[4] Reinhard Jahn,[3] Christian Rosenmund,[3] and Thomas C. Südhof[1]**

[1]Center for Basic Neuroscience, Department of Molecular Genetics, and Howard Hughes Medical Institute, The University of Texas Southwestern Medical Center, Dallas, Texas 75390-9111, Max Planck Institutes for [2]Experimental Medicine and [3]Biophysical Chemistry, 370701 Göttingen, Germany, and [4]Department of Anatomy, Universität des Saarlandes, 66123 Saarbrücken, Germany

**Rab3A, Rab3B, Rab3C, and Rab3D are closely related GTP-binding proteins of synaptic vesicles that may function in neurotransmitter release. We have produced knock-out (KO) mice for Rab3B and Rab3C and crossed them with previously generated Rab3A and 3D knock-out mice to generate double, triple, and quadruple Rab3 knock-out mice. We have found that all single and double Rab3 knock-out mice are viable and fertile. Most triple Rab3 knock-out mice perish whenever Rab3A is one of the three deleted proteins, whereas all triple knock-out mice that express Rab3A are viable and fertile. Finally, all quadruple knock-out mice die shortly after birth. Quadruple Rab3 KO mice initially develop normally and are born alive but succumb to respiratory failure. Rab3-deficient mice display no apparent changes in synapse structure or brain composition except for a loss of rabphilin, a Rab3-binding protein. Analysis of cultured hippocampal neurons from quadruple knock-out mice uncovered no significant change in spontaneous or sucrose-evoked release but an ~30% decrease in evoked responses. This decrease was caused by a decline in the synaptic and the vesicular release probabilities, suggesting that Rab3 proteins are essential for the normal regulation of $Ca^{2+}$-triggered synaptic vesicle exocytosis but not for synaptic vesicle exocytosis as such. Our data show that Rab3 is required for survival in mice and that the four Rab3 proteins are functionally redundant in this role. Furthermore, our data demonstrate that Rab3 is not in itself essential for synaptic membrane traffic but functions to modulate the basic release machinery.**

*Key words:* **membrane fusion; synaptic transmission; GTP-binding proteins; neurotransmitter release; RIM; synaptic vesicles**

## Introduction

Rabs are GTP-binding proteins that are generally involved in regulating membrane traffic (for review, see Darchen and Goud, 2000; Tuvim et al., 2001; Hammer and Wu, 2002; Seabra et al., 2002; Deneka et al., 2003). It seems likely that every vesicular transport reaction involves one or several Rab proteins. Four closely related Rab proteins called Rab3A, Rab3B, Rab3C, and Rab3D are thought to function in mammalian exocytosis (Touchot et al., 1987; Matsui et al., 1988; Zahraoui et al., 1989; Baldini et al., 1992). Rab3 proteins are expressed at highest levels in brain and endocrine tissues but are also found in exocrine glands, adipocytes, and other peripheral tissues (Schlüter et al., 2002). All isoforms of Rab3 appear to be localized on exocytic vesicles. In brain, Rab3 proteins cycle on and off synaptic vesicles in concert with exocytosis (Fischer von Mollard et al., 1991, 1994).

Many, occasionally divergent, functions in exocytosis have been proposed for Rab3 proteins. These functions range from fusion to docking and to the biogenesis of vesicles (for review, see Darchen and Goud, 2000). In transfected pheochromocytoma 12 cells, all four Rab3 proteins strongly decrease $Ca^{2+}$-triggered exocytosis (Chung et al., 1999; Schlüter et al., 2002). Overexpressed Rab3 activates constitutive exocytosis instead of inhibiting regulated exocytosis, indicating that Rab3 inhibits secretion by an indirect effect (Schlüter et al., 2002). Analysis of Rab3A and Rab3D knock-out (KO) mice revealed that each is not required for mouse survival and fertility (Geppert et al., 1994; Riedel et al., 2002). In Rab3A KO mice, the regulation of synaptic vesicle exocytosis is abnormal, but exocytosis is not in itself impaired (Castillo et al., 1997; Geppert et al., 1997). Conversely, Rab3D KO mice exhibit a morphological change in exocrine glands but no significant alteration in overall exocytosis (Riedel et al., 2002). However, these studies only examined individual KOs of Rab3A and Rab3D. The relatively limited phenotype of these KO mice could have been attributable to redundancy among different Rab3 isoforms and may not necessarily reflect discrete functions of Rab3 proteins.

No KOs in multiple Rab3 proteins (or in any other Rab protein) have been analyzed, and it is conceivable that compensation by Rab3B and/or Rab3C confounds the phenotype of Rab3A and Rab3D KO mice. To address this possibility, we have generated and analyzed mice that lack all Rab3 isoforms. Our data demonstrate that Rab3 is essential for mouse survival and that Rab3 isoforms are functionally redundant. However, our data show that Rab3 is not in itself required for exocytosis. In recurrent synapses (autapses) formed by cultured hippocampal neurons,

Received April 27, 2004; revised May 31, 2004; accepted June 2, 2004.

We thank Dr. John Clements for providing a software module in Axograph 4 to deconvolve vesicular release time course; Dr. M. Geppert, Dr. N. Brose, and T. Jo for advice in the early stages of this project; and Dr. H. Riedesel, F. Benseler, Y. Thannhäuser, I. Leznicki, and A. Roth for technical support.

Correspondence should be addressed to Thomas C. Südhof, Center for Basic Neuroscience, University of Texas Southwestern Medical Center, 6000 Harry Hines Boulevard, NA4.118, Dallas, TX 75390-9111. E-mail: Thomas.Sudhof@UTSouthwestern.edu.

O. M. Schlüter's present address: Department of Psychiatry, Stanford University, 1201 Welch Road, Room P152, Stanford, CA 94305.

C. Rosenmund's present address: Department of Neuroscience and Molecular and Human Genetics, Baylor College of Medicine, Room 833E, One Baylor Plaza, Houston, TX 77030.

DOI:10.1523/JNEUROSCI.1610-04.2004

 0270-6474/04/246629-09$15.00/0

deletion of Rab3 induces a discrete reduction in the neurotransmitter release probability without changes in other basic parameters of synaptic vesicle exocytosis. These data suggest that in the brain, Rab3 proteins function as modulators of neurotransmitter release that are not involved in the fundamental machinery of docking and fusion of synaptic vesicles but act as modulators of the release machinery.

## Materials and Methods

*Genomic cloning.* Using a probe from the 5′ end of the rat Rab3C cDNA derived by PCR [primers 337 (GCGGATCCCATATGAGACACGAAGCTCCC) and 338 (GCGGATCCAATCTGAAGCTTGATTCT)], we isolated 22 clones from a λFixII 129SV/J genomic library (Stratagene, La Jolla, CA) and characterized these clones by restriction enzyme mapping and sequencing (Südhof, 1990; Sambrook and Russell, 2001). With specific primers for the Rab3A [primers 500 (GCCATCGATATGGCAAGCACCTCCATGTC) and 501 (GCCATCGATACTCAGTTACCAAGGGGCAG)], Rab3B [primers 475 (GGCTTCAGTGACAGATGG) and 476 (GCGCTGCAGCTTCACACG)], Rab3C [primers 470 (GCGTTTCTGGCAAGGGCA) and 471 (GCGATCGATGCCAACCGT)], and Rab3D [primers 477 (GCGGCATCCGCTAGTGAG) and 478 (GCGGTCATGTCGGTAGACC)] genes, we assigned five clones to the *Rab3A* gene, one clone to the *Rab3B* gene, 10 clones to the *Rab3C* gene, and five clones to the *Rab3D* gene. All clones contained a homologous exon that codes for residues 1–76 in the *Rab3A*, *Rab3B*, and *Rab3D* genes and for residues 9–84 in the *Rab3C* gene (GenBank accession numbers for genes: Rab3A, X72966; Rab3B, AF307514; Rab3C, AF307515; Rab3D, AF263366). This exon was deleted in the new Rab3B and Rab3C KO mice described here, similar to our previously described Rab3A and Rab3D KO mice (Geppert et al., 1994; Riedel et al., 2002).

*Generation and maintenance of Rab3 KO mice.* To delete the homologous 5′ exon of the *Rab3B* and *Rab3C* genes, we constructed similar targeting vectors (see Fig. 1). We cloned an ~9 kb *Not*I–*Bgl*II genomic fragment of clone 6 into the *Not*I and *Bam*HI sites and an ~8 kb *Not*I–*Eco*RV fragment of clone 19 into the *Not*I and *Spe*I sites of pTK-Neo3A (Rosahl et al., 1995) as the long arms of the Rab3B and Rab3C targeting vectors, respectively. We then generated the short arm for the Rab3B vector as a 1.9 kb PCR fragment [primers 540 (CGCATCGATCTCCTACACAGCCATGCAG) and 541 (CGCATCGATGGTACCCTAGTTGTCAATACAAGGTCAAG)], cut it with *Cla*I, and inserted it into the *Cla*I site of pTK-Neo3A containing the long arm. The short arm of the Rab3C vector was generated as an ~7 kb *Not*I–*Kpn*I fragment from clone 14 and inserted into the *Cla*I site of the targeting vector. Electroporation and selection of embryonic day 14.1 (E14.1) mouse embryonic stem cells with the targeting vectors was performed as described previously (Schlüter et al., 2003). Cells were screened for homologous recombination by PCR with the primers 569 (CCTAAGAATCATGTCCTGAGAGATGCC) and 428 and by Southern blotting with outside probes for Rab3B and Rab3C, respectively (see Fig. 1). Two correctly targeted clones each were expanded and injected into C57BL/6J blastocysts. Chimeric offspring were bred to produce homozygous single KO mice that were viable, fertile, and had no obvious phenotype. Multiple KOs were generated by intercrossing the individual lines. Genotyping of mice was performed by PCR: Rab3A wild-type allele, primer 1674 (GGGTCACTGCAAGGCCACTTAGTCAC) versus primer 2440 (CCTCGTTCCTCTTCCGCTACGCAG); Rab3A mutant allele, primer 1673 (CTCACAGAGATCTGCCTCCATCTCCC) versus primer 637 (GGATGCGGTGGGCTCTATGGCTTCTGA); Rab3B wild-type allele, primer 1145 (CTGAAGGAAGGGGTGCTCCAGAGGG) versus primer 1143 (CTGCTCATCATTGGCAACAGCAGCG); Rab3B mutant allele, primer 1145 versus primer 428; Rab3C wild-type allele, primer 2529 (CAGATGTCAGAGACTCAGG) versus primer 2528 (CCCTGCAGATTCCTCATAG); Rab3C mutant allele, primer 1189 (GGATGCTGACGTGTAAAACTGGGATGC) versus primer 428; Rab3D wild-type allele, primer 1149 (GCCATCTCTCCAGCCCTTGTTTGTC) versus primer 1151 (CTCCAGTTATGTAGGCAAGGCTAGCC); and Rab3D mutant allele, primer 1149 versus primer 428. Mice were bred and maintained using standard mouse husbandry procedures (Rosahl et al., 1995; Schlüter et al., 2003).

*Antibodies.* The antibodies used in this study have been described previously (Rosahl et al., 1995; Schlüter et al., 1999, 2002; Fernandez-Chacon and Südhof, 2000; Riedel et al., 2002; Schoch et al., 2002) or were obtained commercially (RIM, Munc13, Mint, and Munc18 antibodies; BD Transduction Laboratories, Lexington, KY).

*Spirometry.* Within 1 hr after birth, mice were placed in a closed recording chamber of defined volume. Pressure changes were detected using a high-sensitivity pressure transducer, and the signals were amplified and digitized using standard acquisition software. Breathing activity was recorded for three consecutive trials at 37°C for a total duration of 5 min.

*Cell culture and electrophysiology.* E19 mouse embryos of Rab3A $^{+/-}$ or Rab3A $^{+/-}$BCD $^{-/-}$ timed matings were delivered by cesarean section. Hippocampi from the entire litter were isolated and cultured in chemically defined media (NBA; Invitrogen, San Diego, CA) supplemented with B27 (Invitrogen) on glial microdot islands (Bekkers and Stevens, 1991; Pyott and Rosenmund, 2002). Islands containing single neurons forming autapses were used after 9–16 d in culture. In all analyses, cultures from the respective KO mice and their littermate control mice were initially established and later analyzed on the same days to avoid culture artifacts (Fernandez-Chacon et al., 2001). Synaptic transmission was recorded in whole-cell configuration under voltage-clamp at −75 to −85 mV (Axopatch 200B; Axon Instruments, Union City, CA) at room temperature (~22–24°C). Synaptic transmission was induced by depolarization to 0 mV for 2 msec, and the triggered synaptic responses were recorded with a sampling rate of 10 kHz filtered at 2 kHz. The standard extracellular recording solution contained (in mM): 140 NaCl, 2.4 KCl, 10 HEPES, 10 glucose, 4 $CaCl_2$, and 4 $MgCl_2$, pH 7.3, with an adjusted osmotic strength of 300 mOsm. Patch pipettes (2.5–3.5 mΩ) were filled with internal solution containing 125 mM K-gluconate, 10 mM NaCl, 4.6 mM $MgCl_2$, 4 mM ATP-$Na_2$, 0.3 mM GTP-$Na_2$, 15 mM creatine phosphate, 20 U/ml phosphocreatine kinase, and 1 mM EGTA, pH 7.3, also adjusted to 300 mOsm. Solutions were applied using a fast-flow application system (Pyott and Rosenmund, 2002). For measurements of spontaneous EPSCs, tetrodotoxin (200 nM; Sankyo, Tokyo, Japan) was added to the standard extracellular recording solution; for measurement of the size of the readily releasable pool, sucrose (500 mM) was added. Dual-component EPSCs (AMPA–NMDA) were measured in the presence of external 2.7 mM $CaCl_2$ and 10 μM glycine and in the absence of $Mg^{2+}$. After a period in which the NMDA receptor-dependent EPSC amplitude had reached a stable baseline, the (+)-5-methyl-10,11-dihydro-5H-dibenzo [a,d] cyclohepten-5,10-imine maleate (MK-801)-dependent (5 μM) blocking rate of the EPSC was measured at a stimulation frequency of 0.33 Hz. The AMPA component was used to normalize for the NMDA-block independent changes in synaptic transmission.

*Data analysis.* Spontaneous EPSCs were monitored for 1–2 min and analyzed with a template detection program (Axograph 4.8; Axon Instruments). The threshold for detection was set to 3.5 times the baseline SD. Captured spontaneous EPSCs of individual cells were averaged to determine amplitude, charge, and decay constant. The vesicular release probability was calculated by dividing the charge of an evoked response by the charge of the burst component of the response to hypertonic sucrose solution of the same cell. Vesicle release time course was determined by deconvolving the EPSC time course with the mean spontaneous EPSC time course using a custom-written software module within Axograph 4.6 (gift from Dr. John Clements, Australian National University, Canberra, Australia). Statistical analyses were performed using Student's $t$ test, and $p < 0.05$ was considered significant. For data fitted with exponential curves, the goodness of fit for each curve fitting was determined by comparing both the $\sigma^2$ and sum-of-squares errors.

*Miscellaneous procedures.* Light and electron microscopy were performed on neurons cultured at high density on a confluent glia feeder layer that were fixed after 12 d in culture with 4% paraformaldehyde and 1% glutaraldehyde in PBS. Electron microscopy, tissue homogenization, immunoblotting, and protein quantifications using $^{125}$I-labeled secondary antibodies and radioactivity measurements on immunoblots were performed as described previously (Rosahl et al., 1995).

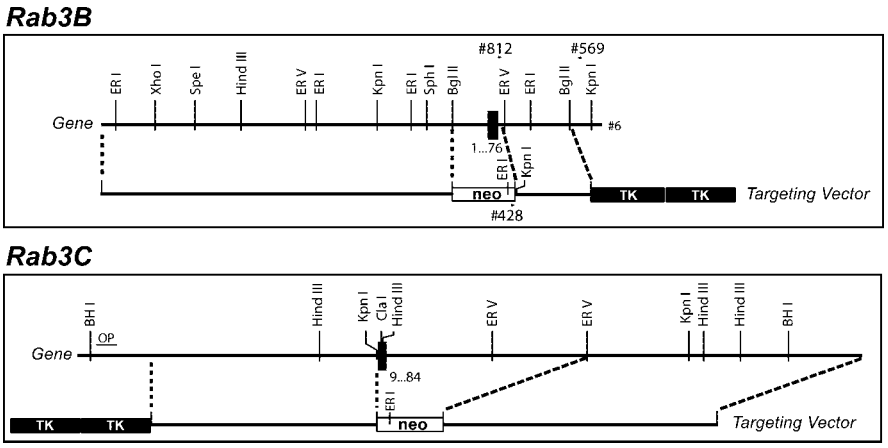


**Figure 1.** Generation of Rab3B and Rab3C knock-out mice. The diagrams depict the structure of the *Rab3B* and *Rab3C* wild-type gene (Gene) and the structure of the targeting vector used for homologous recombination (Targeting Vector). Positions of strategic restriction enzyme sites are indicated, and the residue numbers encoded by the exons (represented as black boxes in the gene structures) are listed below the exons. Localizations of outside probes (OP) and PCR primers (arrows with numbers of letters) are also shown. TK, Thymidine kinase.

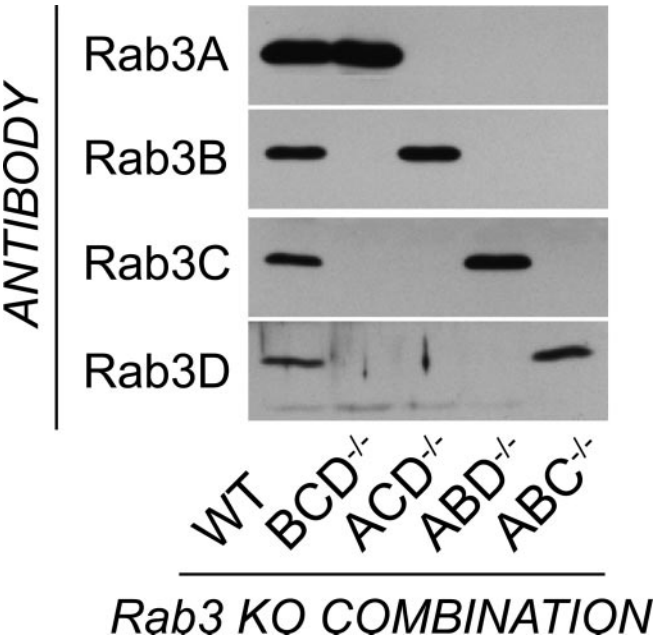


**Figure 2.** Immunoblotting analysis of adult triple Rab3 KO mice. Brain (for Rab3A, Rab3B, and Rab3C) or pituitary (for Rab3D) homogenates from young-adult (6- to 8-week-old) triple KO mice that express only one of the four Rab3 isoforms were examined by immunoblotting. WT, Wild type.

## Results

### Generation of KO mice lacking all four Rab3 isoforms

We produced Rab3B and Rab3C KO mice using the strategy that we previously applied for the generation of Rab3A and Rab3D KO mice (Geppert et al., 1994; Riedel et al., 2002). This strategy deletes the first exon that contains a significant amount of coding sequence. In the *Rab3A*, *Rab3B*, and *Rab3D* genes, this exon specifies residues 1–76, whereas Rab3C has an N-terminal extension and the first exon with a larger stretch of coding sequence encodes residues 9–84 (see Materials and Methods) (Fig. 1). We generated the Rab3B and Rab3C KO mice using standard procedures by electroporating the vectors shown in Figure 1 into embryonic stem cells (Schlüter et al., 1999, 2003) and crossed the resulting KO mice with each other and with the previously generated Rab3A and Rab3D KO mice to obtain mice lacking multiple Rab3 isoforms.

Preliminary analyses indicated that all single and double KO mice and at least some of the triple KO mice were viable and fertile (see systematic analysis below). Therefore, we first aimed to confirm that the KO strategy effectively deleted the various Rab3 proteins. For this purpose, we analyzed all four combinations of triple Rab3 KO mice by immunoblotting with isoform-specific antibodies. We examined brain samples with Rab3A-, Rab3B-, and Rab3C-specific antibodies and pituitary samples with Rab3D-specific antibodies. Pituitary samples were chosen for the Rab3D analysis because Rab3D levels are higher in pituitary than in brain and the Rab3D antibodies exhibit a relatively low affinity, making it difficult to measure Rab3D levels in brain (Schlüter et al., 2002). The blots confirmed that each Rab3 KO resulted in the deletion of the respective Rab3 protein (Fig. 2). Furthermore, the blots demonstrated that in each triple Rab3 KO combination, expression of the remaining Rab3 isoform was not massively enhanced, indicating that there was no compensatory upregulation of the remaining Rab3 isoform when the other three Rab3 proteins were deleted.

### Rab3-deficient mice die at birth

To determine whether deletions of various Rab3 proteins alter the survival of mice, we performed systematic breeding experiments. Surprisingly, in view of the many functions associated with Rab3 in previous studies (Francis et al., 2002; van IJzendoorn et al., 2002), we found that all single and double KO mice lacking various combinations of Rab3 proteins were fully viable, although double KO mice deficient in Rab3A and Rab3C, the most abundant isoforms in the brain, did not attend to their offspring well. To estimate the survival of triple and quadruple KO mice, we performed large-scale matings of double KO mice that lack either Rab3C and Rab3D, Rab3B and Rab3D, or Rab3B and Rab3C and are additionally heterozygous for the remaining two Rab3 genes. As a result, all offspring from these matings will be double homozygotes for the initial two alleles and carry various combinations of alleles for the remaining two Rab3 isoforms. We then compared the genotypes of the surviving adult offspring from these matings with their expected prevalence based on Mendelian inheritance (Fig. 3).

We detected no surviving quadruple Rab3 KO ($ABCD^{-/-}$) mice. For all combinations of triple KO mice, at least some mice survived. Triple KO mice that lack Rab3B, Rab3C, and Rab3D ($BCD^{-/-}$ mice) were fully viable even when the remaining Rab3A gene was a heterozygous mutant. Thus, the four Rab3 isoforms together are essential for survival, but a single wild-type Rab3A allele is sufficient to reverse the lethality of the quadruple Rab3 KO (Fig. 3). In contrast, a heterozygous wild-type Rab3C or Rab3B allele rescued survival of the quadruple KO only by ~50%, whereas homozygous wild-type Rab3C or Rab3B fully rescued survival. A heterozygous Rab3D allele, however, did not support survival (i.e., the Rab3A–RabB–RabC triple KO was 100% lethal when a single mutant allele of Rab3D was present), and homo-

zygous wild-type Rab3D achieved only ~50% survival in triple Rab3A–RabB–RabC KO mice (Fig. 3). These data demonstrate that the various Rab3 isoforms contribute differentially to survival, with Rab3A being the most and Rab3D the least efficient in rescuing the lethality of the quadruple KO mice.

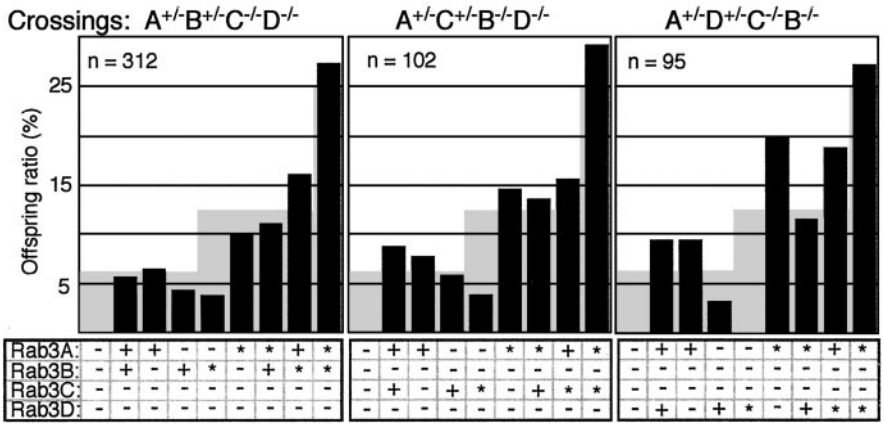


**Figure 3.** Survival analysis of Rab3 KO mice. Mice that were homozygous mutants for two Rab3 isoforms and heterozygous for the remaining two Rab3 isoforms were mated, and the genotypes of surviving adult offspring were determined. The frequency of various genotypes is plotted as percentage of total (gray background indicates the expected frequency based on Mendelian inheritance; asterisks indicate genotypes that exhibit impaired survival). Bottom, Plus signs refer to homozygous wild type, asterisks refer to heterozygous, and minus signs refer to homozygous KO.

### Rab3 KO mice exhibit respiratory failure

Quadruple Rab3 KO mice were born alive and initially reacted to stimuli. However, quadruple KO mice were distressed, lacked stomach milk, and suffered from cyanosis (Fig. 4*A*). The quadruple KO mice died soon after birth but survived longer when placed in a high-oxygen atmosphere (95% $O_2$–5% $CO_2$), indicating that the mice perished because of impaired breathing. Consistent with this hypothesis, whole-body plethysmography showed that newborn quadruple KO mice exhibited a shallow and irregular breathing pattern (Fig. 4*B*). The lungs, however, appeared to be fully inflated as judged by the fact that lungs from newborn quadruple KO mice floated on water (data not shown). Triple KO mice lacking Rab3A displayed a respiratory impairment that was similar to but less severe than that seen in the quadruple KO mice. Triple KO mice that survived despite the respiratory problems during the perinatal period exhibited abnormal cage behavior and were unable to mate. Weight analyses indicated that all triple KO mice in which Rab3A was deleted together with two of the remaining three Rab3 isoforms exhibited a decrease in body weight at 5 weeks of age (Fig. 5). In contrast, even a single wild-type allele of Rab3A not only conferred full survival to triple Rab3 KO mice that lacked all other Rab3 isoforms (Fig. 3) but also rescued the deficit in mating and weight (Fig. 5 and data not shown).

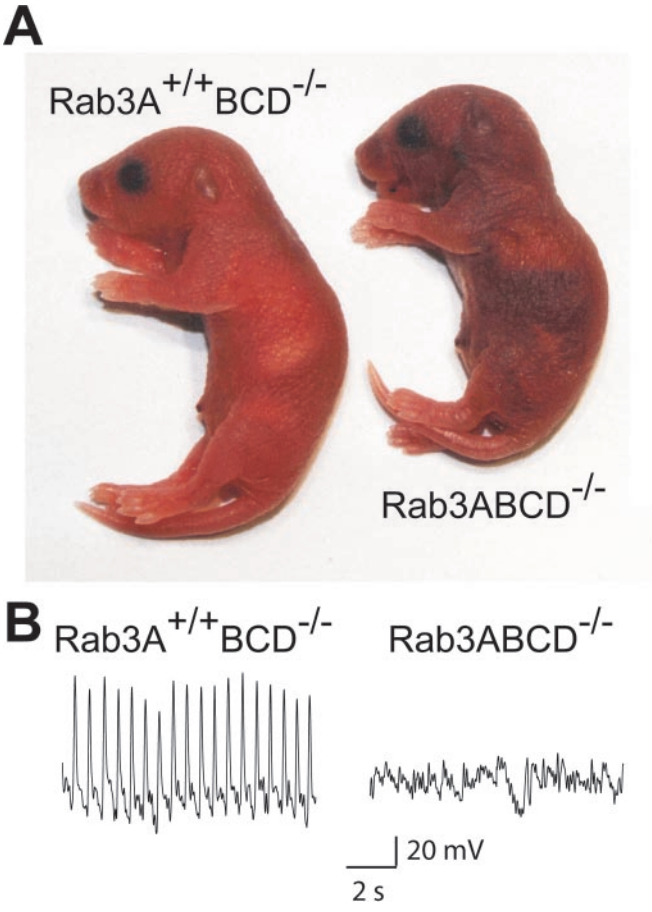


**Figure 4.** Rab3 quadruple KO mice perish from respiratory failure. *A*, Pictures of triple (Rab3A $^{+/+}$–BCD $^{-/-}$) and quadruple Rab3 KO mice (Rab3ABCD $^{-/-}$) at postnatal day 1. Note the lack of milk and cyanosis in the quadruple KO mice. *B*, Respiratory activity measured in Rab3A $^{+/+}$–BCD $^{-/-}$ triple (left) and ABCD $^{-/-}$ quadruple (right) KO mice at birth using whole-body plethysmography.

### Brain composition of Rab3 KO mice

We next asked whether deletion of Rab3 proteins caused a major alteration in brain structure or composition. We uncovered no striking abnormalities by microscopy (data not shown). To detect potential changes in brain composition, we quantitated the levels of 26 neuronal proteins in newborn Rab3 quadruple KO mice using littermate triple KO mice expressing Rab3A as a control, because these triple KO mice exhibit no change in weight, fertility, or survival. We detected no significant change in any protein except for rabphilin (Table 1). Rabphilin is a synaptic vesicle protein and putative Rab3 effector that requires Rab3 for binding to synaptic vesicles (Li et al., 1994). However, another putative Rab3 effector, RIM1$\alpha$ (Wang et al., 1997), was not altered. Because synaptic proteins are expressed at relatively low levels in the newborn brain (Daly and Ziff, 1997), the magnitude of the change in rabphilin is difficult to investigate in detail at this age. We therefore examined the levels of rabphilin in older surviving triple Rab3 KO mice (Fig. 6). In the most severely affected Rab3 KO combinations (triple KO mice containing only a single wild-type Rab3B or Rab3C allele), rabphilin decreased >75%, consistent with the notion that the stability of rabphilin in mice completely depends on Rab3.

### Spontaneous neurotransmitter release in Rab3 knock-out mice

To examine the properties of synapses from Rab3 KO mice, we cultured hippocampal neurons from fetal mice (embryonic day

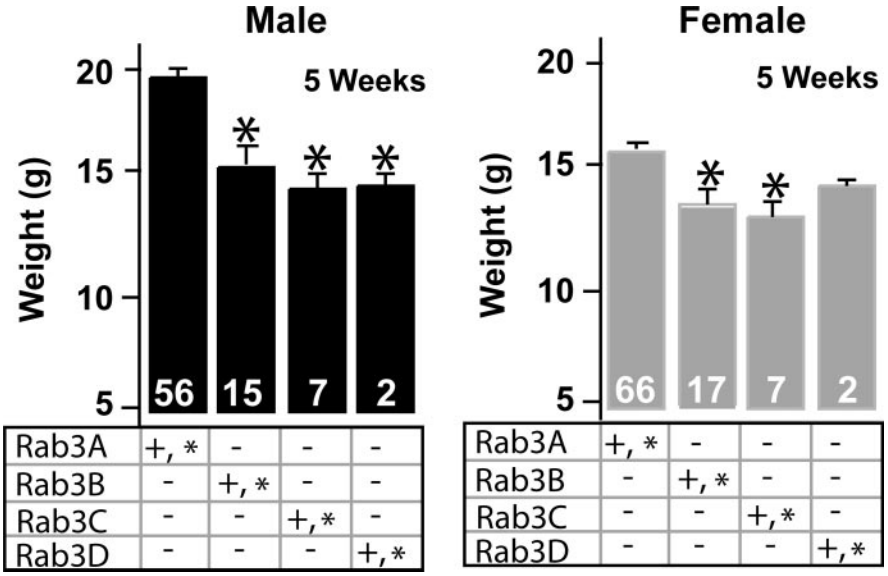


**Figure 5.** Body weights of surviving Rab3 triple KO mice. Weights of male and female 5-week-old mice that are triple KO for three Rab3 isoforms and heterozygous or wild type for the fourth. An asterisk indicates a statistically significant difference from Rab3A $^{+/-}$–BCD $^{-/-}$ or Rab3A $^{+/+}$–BCD $^{-/-}$ at $p < 0.05$; the number of individual mice is given at the bottom of each bar. Bottom, Plus signs refer to homozygous wild type, asterisks refer to heterozygous, and minus signs refer to homozygous KO.

**Table 1. Protein levels in total brain homogenates of postnatal day 1 mice**

| Protein | Rab3ABCD $^{-/-}$ | Rab3A $^{+/+}$ –BCD $^{-/-}$ | Antibody |
|---|---|---|---|
| $\beta$-Actin | 99.4 ± 1.9 | 100 ± 2.3 | Actin |
| $\alpha$-Synuclein | 97.7 ± 6.1 | 100 ± 3.9 | Syf |
| $\alpha$-Tubulin | 101.3 ± 0.8 | 100 ± 1.1 | Tub |
| $\beta$-Synuclein | 102.4 ± 9.9 | 100 ± 15.9 | U1128 |
| CAPS I | 94.9 ± 6.7 | 100 ± 6.8 | CAPS |
| CSP | 102.9 ± 5.8 | 100 ± 6.7 | CSP |
| GDI | 101.2 ± 3.2 | 100 ± 1.6 | CI81.2 |
| Mint | 101 ± 3.5 | 100 ± 3.4 | P932 |
| Munc13-1 | 108.9 ± 4.2 | 100 ± 2.5 | 40 |
| Munc13-2 | 100.9 ± 9.2 | 100 ± 6.3 | 44 |
| Munc18 | 102.8 ± 3.1 | 100 ± 1.2 | I370 |
| Neuroligin I | 103.2 ± 2.8 | 100 ± 2.4 | 4C12 |
| Rab3A | 0.5 ± 0.1 | 100 ± 3.6 | CI42.2 |
| Rab5 | 102.4 ± 1.9 | 100 ± 1.6 | CI621.3 |
| Rabaptin | 100.9 ± 4.6 | 100 ± 2.2 | R321 |
| Rabphilin | 56.6 ± 4.4 | 100 ± 2.7 | I734 |
| RIM1 | 105.9 ± 3.5 | 100 ± 8.3 | RIM |
| Rim1$\alpha$ | 99.3 ± 8.1 | 100 ± 2.4 | U952 |
| Rim2$\beta$ | 96.1 ± 12.7 | 100 ± 3.3 | U952 |
| SCAMP1 | 98.9 ± 5.3 | 100 ± 1.9 | P936 |
| SCAMP5 | 110.3 ± 7.7 | 100 ± 7.5 | SCAMP5 |
| SGT2 | 108.1 ± 6.5 | 100 ± 5.1 | SGT2 |
| SNAP-25 | 101.3 ± 0.7 | 100 ± 1.5 | CI71.2 |
| Synapsin I | 102.7 ± 2.2 | 100 ± 2.2 | E028 |
| Synaptobrevin 2 | 98.2 ± 1.3 | 100 ± 0.7 | CI69.1 |
| Synaptogyrin | 100.5 ± 2.2 | 100 ± 3.9 | P925 |
| Synaptophysin 1 | 105.7 ± 5.1 | 100 ± 4 | 580 |
| Synaptotagmin 1 | 100 ± 3.3 | 100 ± 3.9 | V216 |

Proteins in the brains of newborn mice (postnatal day 1) were measured by quantitative immunoblotting using internal standards and $^{125}$I-labeled secondary antibodies and phosphorimager detection as described previously (Rosahl et al., 1995; Schlüter et al., 1999). CAPS, Calcium-activated protein of secretion; CSP, cystein string protein; GDI, GDP-dissociation inhibitor; SCAMP, secretory carrier membrane protein 1; SGT2, small glutamine-rich tetratricopeptide repeat-containing protein; SNAP, soluble *N*-ethylmaleimide-sensitive factor attached protein.

19) on microislands of astrocytes, conditions that induce formation of autapses (Bekkers and Stevens, 1991). In these and the following experiments, we compared neurons derived from quadruple ABCD $^{-/-}$ KO mice with control neurons derived from littermate triple BCD $^{-/-}$ KO mice because the weight and survival measurements (Figs. 3, 5) showed that Rab3A fully compensates for the loss of the other three Rab3 isoforms. In some experiments, we also compared Rab3A $^{-/-}$ KO neurons with wild-type neurons to exclude the possibility that a particular phenotype is solely induced by deletion of Rab3A. It would have been preferable to use littermate wild-type controls for quadruple KO mice, but this was impractical because only 1 in 256 offspring from quadruple heterozygous breedings will be homozygous mutant or wild type. All experiments were performed with neurons from newborn littermate mice that were studied on the same days to exclude interexperimental variations between cultures and analysis days (Fernandez-Chacon et al., 2001).

Immunofluorescence analysis showed that synapses were formed at a similar density in cultured neurons from various wild-type and Rab3 KO mice (data not shown). These synapses, as viewed by electron microscopy, exhibited typical features with abundant presynaptic vesicles, including vesicles that are docked at the active zone (Fig. 7). Using whole-cell recordings, we found that the frequency of spontaneous release events and their properties (e.g., amplitudes, rise times, duration, and decay kinetics) were indistinguishable between quadruple KO neurons that lack all Rab3 isoforms and control triple KO neurons that lack Rab3A (Fig. 8). Thus, deletion of Rab3 does not cause major alterations in synapse formation or synaptic properties such as the size of synaptic vesicles, filling of synaptic vesicles with neurotransmitters, number of postsynaptic receptors, or kinetics of neurotransmitter release.

### Evoked neurotransmitter release in Rab3 knock-out mice

We next examined whether synaptic responses evoked by presynaptic action potentials are altered in Rab3-deficient synapses. We found that the size of the EPSC induced by action potentials was ~30% smaller in quadruple KO mice than in control littermates (Fig. 9). In contrast, mice lacking Rab3A alone exhibited no decline in the EPSC compared with wild-type littermates, indicating that the reduction in EPSC size in quadruple KO mice is not solely attributable to deletion of Rab3A (Rab3A $^{+/+}$, 4.3 ± 0.7 nA, $n = 22$; Rab3A $^{-/-}$, 4.9 ± 0.7 nA, $n = 14$; $p = 0.60$). In hippocampal autapses stimulated at room temperature, ~80% of release is fast and synchronous (time constant, ~2 msec), whereas ~20% of release is delayed and asynchronous (time constant, ~20 msec). To analyze whether loss of Rab3 alters the time course of vesicle fusion, we deconvolved the time course of evoked responses and fitted it to a two-exponential function (Fig. 9*B*). The observed time constants (BCD $^{-/-}$, $\tau_{fast}$, 1.7 ± 0.3 msec, $\tau_{slow}$, 19 ± 4 msec, $n = 25$; ABCD $^{-/-}$, $\tau_{fast}$, 1.9 ± 0.4 msec, $\tau_{slow}$, 17 ± 5 msec, $n = 26$) and their relative weights (BCD $^{-/-}$, $\tau_{fast}$, 73 ± 6%, $\tau_{slow}$, 25 ± 4%; ABCD $^{-/-}$, $\tau_{fast}$, 77 ± 4%, $\tau_{slow}$, 21 ± 3%) were not significantly altered in quadruple KO mice, indicating that the decrease in EPSC size was not associated with a change in the kinetics of release.

Is the decrease in evoked responses in the quadruple KO neurons attributable to a decrease in the number of release-ready

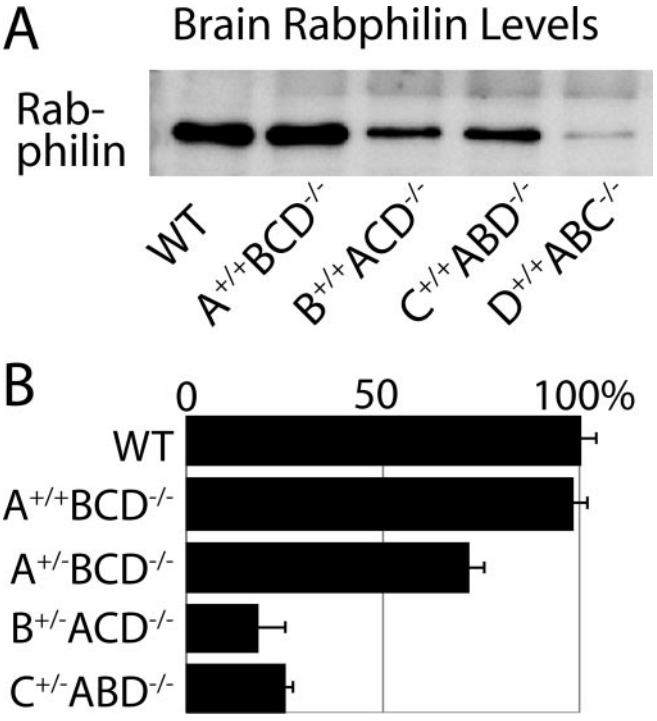


**Figure 6.** Rabphilin levels in brains from Rab3 KO mice. *A*, Immunoblots of rabphilin in brains from the indicated adult triple KO mice. *B*, Proteins levels were quantified in adult mice by immunoblotting using $^{125}$I-labeled secondary antibodies with phosphorimager detection and are plotted as percentage of the wild-type control. See Table 1 for quantifications of protein levels in newborn quadruple KO mice. WT, Wild type.

vesicles or to an impairment in $Ca^{2+}$ triggering of release? To distinguish between these possibilities, we measured the readily releasable pool of synaptic vesicles. We recorded synaptic responses to hypertonic sucrose (Fig. 10*A*) that acts by an unknown, $Ca^{2+}$-independent mechanism to trigger exocytosis of primed vesicles (Rosenmund and Stevens, 1996). Responses to hypertonic sucrose were slightly smaller in quadruple KO neurons than in control KO neurons, but the difference was not statistically significant (Fig. 10*B*). These findings suggest that the decrease in evoked synaptic responses in Rab3-deficient synapses is not caused by a significant reduction in the number of primed vesicles.

### Deletion of Rab3 decreases the synaptic and the vesicular release probability

We next asked whether the release probability is decreased in Rab3-deficient neurons. To test this, we evaluated the vesicular release probability (the probability of a given vesicle to fuse when triggered by an action potential) as the ratio of vesicles released by an action potential to the vesicles released by hypertonic sucrose. As shown in the cumulative probability plot (Fig. 11*A*), the distribution of release probabilities as measured from 141 individual triple deficient and 165 individual quadruple KO neurons covered a wide range of release probabilities, yet shifted uniformly to lower probabilities in the quadruple KO.

Using an independent approach to measure release probability, we also monitored NMDA receptor-mediated synaptic responses to low-frequency stimulation (0.33 Hz) in the presence of MK-801. MK-801 is an irreversible NMDA receptor antagonist that only blocks activated receptors; thus, the progressive block rate of EPSCs by MK-801 during ongoing stimulation is a direct measure of the synaptic release probability (Hessler et al., 1993; Rosenmund et al., 1993). The rate of the MK-801-induced EPSC

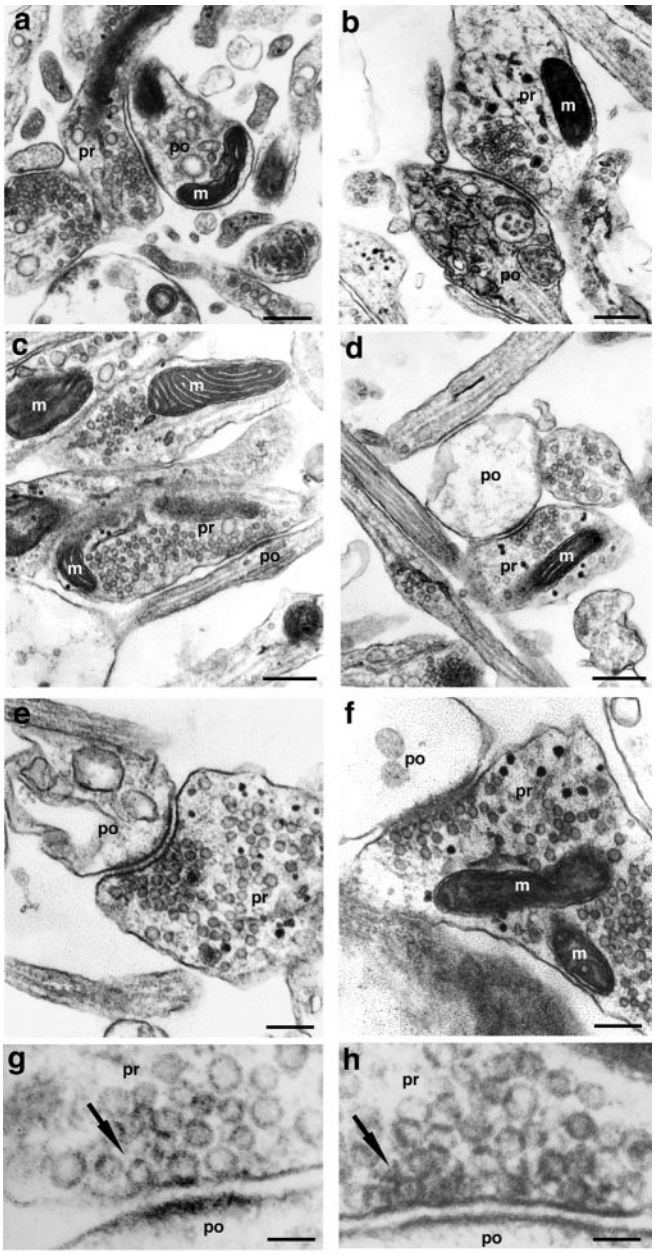


**Figure 7.** Structure of synapses formed by cultured neurons from Rab3 KO mice. Electron micrographs of synapses formed in cultured hippocampal neurons from quadruple Rab3ABCD $^{-/-}$ KO mice (*a*, *c*, *e*, *g*) and triple Rab3BCD $^{-/-}$ (*b*, *d*, *f*, *g*). pr, Presynaptic compartments; po, postsynaptic compartments; m, mitochondria. Arrows in *g* and *h* point to docked vesicles in a high-magnification view of the synapse. Scale bars: *a*–*d*, 300 nm; *e*, *f*, 200 nm; *g*, *h*, 80 nm.

block was significantly slower in quadruple KO neurons than in control KO neurons (Fig. 11*B*), confirming that deletion of Rab3 causes a reduced synaptic release probability. To determine whether synapses with different release probabilities were uniformly affected or only a subset of synapses was preferentially impaired, we tested whether the MK-801 inhibition curve in quadruple KO neurons could be converted into that of the control by simple transformation of the *x*-axis (Fernandez-Chacon et al., 2001). Indeed, an 1.8-fold decrease in the scale of the *x*-axis converted the quadruple KO curve into the triple KO curve, indicating a homogeneous ~40% decrease in synaptic release probability in the quadruple KO neurons (Fig. 11*B*, inset). Because the

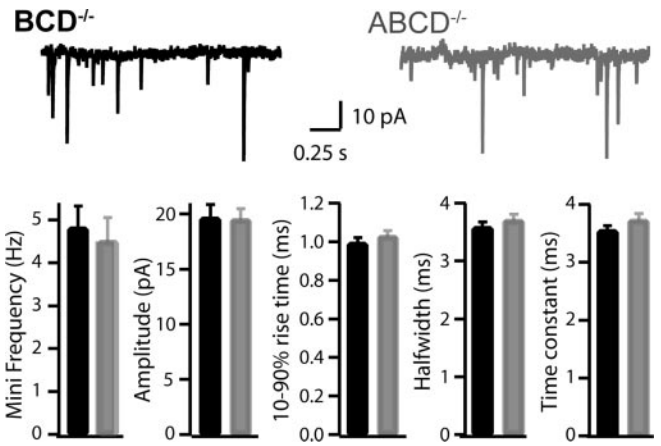


**Figure 8.** Spontaneous synaptic events in Rab3 KO mice. Representative traces of spontaneous synaptic events (top) and summary of the properties of spontaneous events (bottom) recorded in neurons from triple Rab3BCD $^{-/-}$ and quadruple Rab3ABCD $^{-/-}$ KO mice. Recordings were performed in cultured hippocampal neurons that had formed autapses ($n = 39$ for both genotypes).

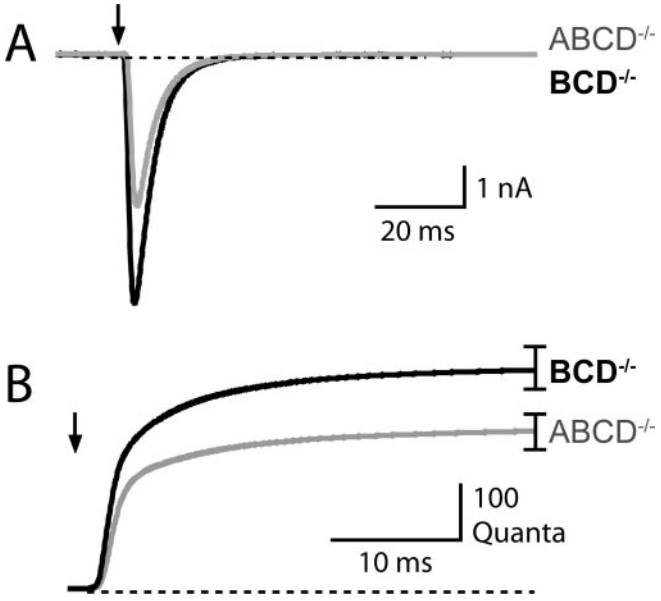


**Figure 9.** Evoked synaptic responses in Rab3 KO mice. *A*, Representative traces of evoked EPSCs triggered by somatic depolarization (arrow, from −70 to 0 mV for 2 msec). Stimulation current was blanked for display purposes. *B*, Mean cumulative vesicle release from triple (BCD $^{-/-}$; $n = 124$) and quadruple (ABCD $^{-/-}$; $n = 165$) KO neurons. Error bars indicate SE ($p < 0.01$). The quantal content and vesicular release time course were calculated by deconvolving synaptic responses with the mean spontaneous synaptic response. The time course of release was determined from a subset of these data (BCD $^{-/-}$, $n = 27$; ABCD $^{-/-}$, $n = 29$) by fitting the curves to a two-exponential function and was not significantly different between the two genotypes. The dashed lines represent baseline current (*A*) and baseline release rate (*B*), respectively.

only difference between the triple and quadruple KO neurons is the presence or absence of Rab3A, it is possible that the quadruple KO phenotype is caused by deletion of Rab3A alone. However, consistent with previous studies (Geppert et al., 1994, 1997; Schoch et al., 2002), we detected no measurable difference in the release probability between Rab3A $^{-/-}$ KO neurons and wild-type controls (data not shown), confirming that the quadruple KO phenotype is indeed a synthetic effect of the deletion of all Rab3 isoforms.

## Discussion

Rab3 proteins are abundant GTP-binding proteins of synaptic vesicles and other secretory organelles. Mammals express four differentially distributed Rab3 isoforms: Rab3A, Rab3B, Rab3C, and Rab3D. Although a large number of experiments using *in vitro* approaches tie Rab3 proteins to many different functions (Chung et al., 1999; Francis et al., 2002; van IJzendoorn et al., 2002), the precise role and the potential redundancy of Rab3 proteins have not been clarified. To obtain a complete assessment of the essential functions of Rab3 proteins, we have generated and analyzed KO mice that are deficient in two, three, or all four Rab3 isoforms (Figs. 1, 2). Our results demonstrate that no deletion of an individual Rab3 protein or any combination of two Rab3 proteins causes a major change in the survival of mice. Deletion of three Rab3 proteins, in contrast, was deleterious when Rab3A was one of the three deleted proteins but had no apparent effect when Rab3A was still expressed (Figs. 3–5). Deletion of all four Rab3 proteins, moreover, caused complete lethality of the KO mice at birth. These data document that no individual Rab3 protein performs an isolated separate function that is required for reproduction or survival. For example, Rab3A or Rab3B KO mice exhibited no apparent decrease in weight or fertility, indicating that contrary to previous hypotheses, these proteins are not required for a fundamental gastrointestinal or reproductive function (Michaut et al., 2000). Most importantly, our data show that the four Rab3 proteins are functionally redundant, despite their differential distributions.

We next examined why the Rab3 KO mice die. The major cause of death appeared to be irregular respiratory activity, although other factors such as dehydration may have contributed. Irregular respiratory activity points to a defect of the respiratory circuits in the brainstem. This, together with the preferential localization of Rab3 proteins to synaptic vesicles, indicates a possible impairment in synaptic neurotransmitter release. To study this, we examined the structure and composition of the brain and used cultured hippocampal neurons to test synaptic function. We detected no obvious developmental abnormalities, changes in synapse structure, or alterations in brain composition (Figs. 6, 7; Table 1). Although this does not exclude a subtle developmental effect of the Rab3 KO, this observation argues against a major developmental aberration.

In a final set of experiments, we studied synaptic transmission in the quadruple KO mice. Surprisingly, we found that synaptic vesicle exocytosis exhibited a discrete impairment of release that manifests as an ~30% decrease in evoked responses (Figs. 8–10). This decrease was attributable to a decline in the synaptic and vesicular release probability, indicating that deletion of Rab3 impairs $Ca^{2+}$ triggering of release (Fig. 11). Noticeably, we observed no significant impairment of synaptic vesicle biogenesis, transport, docking, or priming. These data confirm that at least for synaptic vesicle exocytosis, Rab3 performs a modulatory function that acts at the fusion step.

How does a 30% decrease in release translate into respiratory failure and a 100% lethality in quadruple Rab3 KO mice? At least two hypotheses that are not mutually exclusive can be advanced to explain the origin of the respiratory failure in the Rab3 KO mice: (1) In the present study, our experiments were restricted to measuring excitatory responses in cultured hippocampal neurons elicited by low-frequency stimulation. However, readouts of synaptic networks depend on the precise synaptic properties of the neurons *in situ* and the balance between excitation and inhibition. Considering the fact that the release properties of synapses

are very heterogeneous and that our data indicate a selective role in shaping release properties, different synapse types may be regulated differentially by Rab3 proteins. This possibility is supported by the divergent effects of the Rab3A deletion on two different excitatory synapses in the hippocampus, Schaffer collateral–commissural fiber synapses (Geppert et al., 1994, 1997) versus mossy fiber synapses (Castillo et al., 1997). If different synapses are differentially altered by the Rab3 deletion, then the balance between excitation and inhibition in respiratory synaptic circuits may have been lost, resulting in abnormal regulation of respiration. (2) We have not examined endocrine cells that are known to have high levels of Rab3 proteins. Changes in endocrine regulation could indirectly cause respiratory changes and lethality. Future studies will have to investigate these possibilities.

Previous studies have examined the phenotype of mice lacking the Rab3 GDP–GTP exchange factor (Rab3-GEF) (Yamaguchi et al., 2002) and the Rab3 effectors rabphilin (Schlüter et al., 1999) and RIM1$\alpha$ (Calakos et al., 2004). Rab3-GEF-deficient mice exhibit similarities to the Rab3-deficient mice we describe here, including a selective decrease in $Ca^{2+}$-evoked release with a normal size of the readily releasable pool. Rab3-GEF-deficient mice also fail to display morphological changes in the synapse, although they exhibit, different from the Rab3-deficient synapses, changes in the frequency of spontaneous miniature release events (Yamaguchi et al., 2002). The similarity of the Rab3-GEF and Rab3 KO mice strongly supports the notion that Rab3-GEF primarily functions to activate Rab3 proteins. This is an important conclusion, because the Rab3-GEF contains a "death domain" and was independently described as "DENN" (differentially expressed in normal vs neoplastic) (Chow and Lee, 1996) and "MADD" (mitogen-activated protein kinase-activating death domain protein) (Zhang et al., 1998), proteins that bind to the p55 tumor necrosis factor receptor type 1. As DENN and MADD, the Rab3-GEF has been implicated in regulating apoptosis (Al-Zoubi et al., 2001), whereas the similarity of the Rab3-GEF KO phenotype with that of the quadruple Rab3 KO phenotype rather suggests a role in neurotransmitter release.

Different from the Rab3-GEF knock-out mice, knock-out mice for the Rab3 effectors rabphilin and RIM1$\alpha$ exhibit either no phenotype (Rabphilin) (Schlüter et al., 1999) or a severe phenotype with a partial overlap with that of Rab3 (RIM1$\alpha$) (Schoch et al., 2002; Calakos et al., 2004). In Rab3 and RIM1$\alpha$ knock-outs, spontaneous release events are unaltered, but evoked release is impaired. However, RIM1$\alpha$-deficient synapses suffer from an ~50% decrease in the readily releasable pool (Calakos et al., 2004), whereas in the Rab3-deficient synapses, the readily releasable pool is normal. The more extensive phenotype of the RIM1$\alpha$ KO mice is probably attributable to the fact that RIM1$\alpha$ interacts with multiple other active zone proteins at the synapse (Schoch et al., 2002).

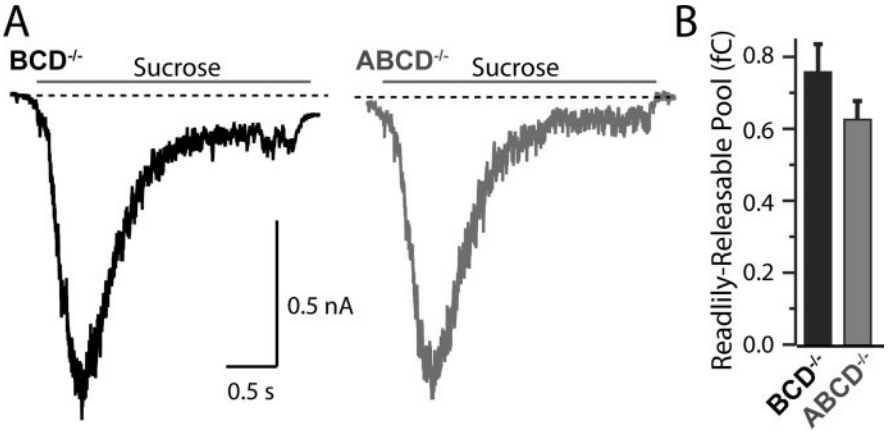


**Figure 10.** Response to sucrose stimulation in Rab3-deficient synapses. *A*, Representative traces of synaptic responses to hypertonic sucrose. The dashed lines indicate baseline. *B*, Average size of sucrose-evoked synaptic responses ($n = 141$ and 165 for BCD $^{-/-}$ and ABCD $^{-/-}$ neurons, respectively). The decrease in the quadruple KO synapses is not statistically significant ( $p = 0.16$).

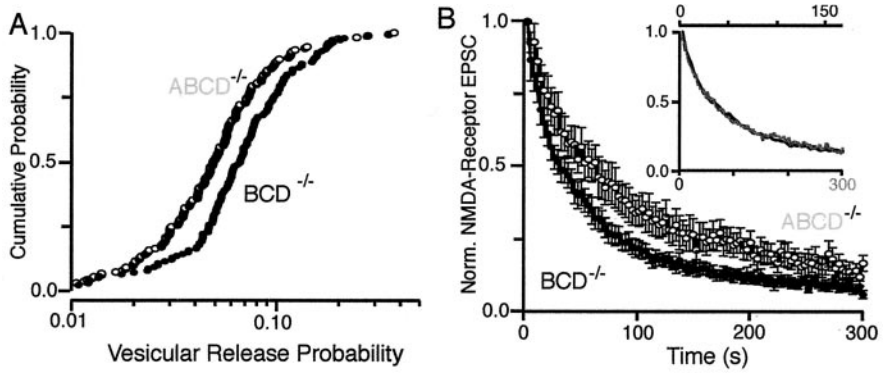


**Figure 11.** Decreased release probability in Rab3 KO neurons. *A*, Cumulative plot of the vesicular release probability. Individual values were calculated as the ratio of the synaptic charge of action potential-induced to sucrose-induced EPSCs for individual neurons. *B*, Stimulus-dependent progressive block of EPSCs with the irreversible NMDA-type glutamate receptor antagonist MK-801. The normalized NMDA receptor-dependent component of the EPSCs was plotted (see Materials and Methods for details). Synaptic responses were evoked at 0.33 Hz ($n = 13$ cells of 3 cultures). Inset, Transformation of the data by expanding the time axis of the Rab3BCD $^{-/-}$ 1.8-fold causes complete superposition of the two curves.

Our data thus show that Rab3 joins the ranks of proteins that are present at high concentration at the synapse but primarily perform a regulatory function, similar to synapsins, SV2 (synaptic vesicle protein 2), and other synaptic vesicle proteins. The selective requirement for Rab3 in modulating fusion uncovered here is unusual for a Rab protein. The requirement suggests that the synapse may have exploited a protein family normally used in a number of basic membrane trafficking functions (e.g., docking, transport, and budding) for a specialized role. Among others, this indicates that other Rab proteins likely play central roles in synaptic vesicle exocytosis. Identification of these Rabs forms one of the major challenges for the future.

## References

Al-Zoubi AM, Efimova EV, Kaithamana S, Martinez O, El-Idrissi Mel-A, Dogan RE, Prabhakar BS (2001) Contrasting effects of IG20 and its splice isoforms, MADD and DENN-SV, on tumor necrosis factor alpha-induced apoptosis and activation of caspase-8 and -3. J Biol Chem 276:47202–47211.

Baldini T, Hohl H, Lin Y, Lodish HF (1992) Cloning of a Rab3 isotype predominantly expressed in adipocytes. Proc Natl Acad Sci USA 89:5049–5052.

Bekkers JM, Stevens CF (1991) Excitatory and inhibitory autaptic currents in isolated hippocampal neurons maintained in cell culture. Proc Natl Acad Sci USA 88:7834–7836.

Calakos N, Schoch S, Südhof TC, Malenka RC (2004) Multiple roles for the active zone protein RIM1$\alpha$ in late stages of neurotransmitter release. Neuron 42:889–896.

Castillo PE, Janz R, Südhof TC, Tzounopoulos T, Malenka RC, Nicoll RA (1997) The synaptic vesicle protein Rab3 is essential for mossy fiber long term potentiation in the hippocampus. Nature 388:590–593.

Chow VT, Lee SS (1996) DENN, a novel human gene differentially expressed in normal and neoplastic cells. DNA Seq 6:263–273.

Chung SH, Joberty G, Gelino EA, Macara IG, Holz RW (1999) Comparison of the effects on secretion in chromaffin and PC12 cells of Rab3 family members and mutants. Evidence that inhibitory effects are independent of direct interaction with Rabphilin. J Biol Chem 274:18113–18120.

Daly C, Ziff EB (1997) Post-transcriptional regulation of synaptic vesicle protein expression and the developmental control of synaptic vesicle formation. J Neurosci 17:2365–2375.

Darchen F, Goud B (2000) Multiple aspects of Rab protein action in the secretory pathway: focus on Rab3 and Rab6. Biochimie 82:375–384.

Deneka M, Neeft M, van der Sluijs P (2003) Regulation of membrane transport by rab GTPases. Crit Rev Biochem Mol Biol 38:121–142.

Fernandez-Chacon R, Südhof TC (2000) Novel SCAMPs lacking NPF repeats: ubiquitous and synaptic vesicle-specific forms implicate SCAMPs in multiple membrane-trafficking functions. J Neurosci 20:7941–7950.

Fernandez-Chacon R, Königstorffer A, Gerber SH, Garcia J, Matos MF, Stevens CF, Brose N, Rizo J, Rosenmund C, Südhof TC (2001) Synaptotagmin I functions as a $Ca^{2+}$-regulator of release probability. Nature 410:41–49.

Fischer von Mollard G, Südhof TC, Jahn RA (1991) A small GTP-binding protein dissociates from synaptic vesicles during exocytosis. Nature 349:79–81.

Fischer von Mollard G, Stahl B, Khoklatchev A, Südhof TC, Jahn R (1994) Rab3C is a synaptic vesicle protein that dissociates from synaptic vesicles after stimulation of exocytosis. J Biol Chem 269:10971–10974.

Francis SC, Sunshine C, Kirk KL (2002) Coordinate regulation of catecholamine uptake by rab3 and phosphoinositide 3-kinase. J Biol Chem 277:7816–7823.

Geppert M, Bolshakov VY, Siegelbaum SA, Takei K, De Camilli P, Hammer RE, Südhof TC (1994) The role of Rab3A in neurotransmitter release. Nature 369:493–497.

Geppert M, Goda Y, Stevens CF, Südhof TC (1997) Rab3A regulates a late step in synaptic vesicle fusion. Nature 387:810–814.

Hammer III JA, Wu XS (2002) Rabs grab motors: defining the connections between Rab GTPases and motor proteins. Curr Opin Cell Biol 14:69–75.

Hessler NA, Shirke AM, Malinow R (1993) The probability of transmitter release at a mammalian central synapse. Nature 366:569–572.

Li C, Takei K, Geppert M, Daniell L, Stenius K, Chapman ER, Jahn R, De Camilli P, Südhof TC (1994) Synaptic targeting of rabphilin-3A, a synaptic vesicle $Ca^{2+}$/phospholipid-binding protein, depends on rab3A/3C. Neuron 13:885–898.

Matsui Y, Kikuchi A, Kondo J, Hishida T, Teranishi Y, Takai Y (1988) Nucleotide and deduced amino acid sequences of a GTP-binding protein family with molecular weights of 25,000 from bovine brain. J Biol Chem 263:11071–11074.

Michaut M, Tomes CN, De Blas G, Yunes R, Mayorga LS (2000) Calcium-triggered acrosomal exocytosis in human spermatozoa requires the coordinated activation of Rab3A and *N*-ethylmaleimide-sensitive factor. Proc Natl Acad Sci USA 97:9996–10001.

Pyott SJ, Rosenmund C (2002) The effects of temperature on vesicular supply and release in autaptic cultures of hippocampal neurons. J Physiol (Lond) 539:523–535.

Riedel D, Antonin W, Fernandez-Chacon R, Alvarez de Toledo G, Jo T, Geppert M, Valentijn JA, Valentijn K, Jamieson JD, Südhof TC, Jahn R (2002) Rab3D is not essential for exocrine exocytosis. Mol Cell Biol 22:6487–6497.

Rosahl TW, Spillane D, Missler M, Herz J, Selig DK, Wolff JR, Hammer RE, Malenka RC, Südhof TC (1995) Essential functions of synapsins I and II in synaptic vesicle regulation. Nature 375:488–493.

Rosenmund C, Stevens CF (1996) Definition of the readily releasable pool of vesicles at hippocampal synapses. Neuron 16:1197–1207.

Rosenmund C, Clements JD, Westbrook GL (1993) Nonuniform probability of glutamate release at a hippocampal synapse. Science 262:754–757.

Sambrook J, Russell DW (2001) Molecular cloning, a laboratory manual, Ed 3. Cold Spring Harbor, NY: Cold Spring Harbor Laboratory.

Schlüter OM, Schnell E, Verhage M, Tzounopoulos T, Nicoll RA, Janz R, Malenka RC, Geppert M, Südhof TC (1999) Rabphilin knock-out mice reveal that rabphilin is not required for rab3 function in regulating neurotransmitter release. J Neurosci 19:5834–5846.

Schlüter OM, Khvotchev M, Jahn R, Südhof TC (2002) Localization versus function of Rab3 proteins: evidence for a common regulatory role in controlling fusion. J Biol Chem 277:40919–40929.

Schlüter OM, Fornai F, Alessandri MG, Takamori S, Geppert M, Jahn R, Südhof TC (2003) Role of $\alpha$-synuclein in MPTP-induced Parkinsonism in mice. Neuroscience 118:985–1002.

Schoch S, Castillo PE, Jo T, Mukherjee K, Geppert M, Wang Y, Schmitz F, Malenka RC, Südhof TC (2002) RIM1$\alpha$ forms a protein scaffold for regulating neurotransmitter release at the active zone. Nature 415:321–326.

Seabra MC, Mules EH, Hume AN (2002) Rab GTPases, intracellular traffic and disease. Trends Mol Med 8:23–30.

Südhof TC (1990) The structure of the human synapsin I gene and protein. J Biol Chem 265:7849–7852.

Touchot N, Chardin P, Tavitian A (1987) Four additional members of the ras gene superfamily isolated by an oligonucleotide strategy: molecular cloning of YPT-related cDNAs from a rat brain library. Proc Natl Acad Sci USA 84:8210–8214.

Tuvim MJ, Adachi R, Hoffenberg S, Dickey BF (2001) Traffic control: Rab GTPases and the regulation of interorganellar transport. News Physiol Sci 16:56–61.

van IJzendoorn SC, Tuvim MJ, Weimbs T, Dickey BF, Mostov KE (2002) Direct interaction between Rab3b and the polymeric immunoglobulin receptor controls ligand-stimulated transcytosis in epithelial cells. Dev Cell 2:219–228.

Wang Y, Okamoto M, Schmitz F, Hofmann K, Südhof TC 1997) Rim is a putative Rab3 effector in regulating synaptic vesicle fusion. Nature 338:593–598.

Yamaguchi K, Tanaka M, Mizoguchi A, Hirata Y, Ishizaki H, Kaneko K, Miyoshi J, Takai Y (2002) A GDP/GTP exchange protein for the Rab3 small G protein family up-regulates a postdocking step of synaptic exocytosis in central synapses. Proc Natl Acad Sci USA 99:14536–14541.

Zahraoui A, Touchot N, Chardin P, Tavitian A (1989) The human Rab genes encode a family of GTP-binding proteins related to yeast YPT1 and SEC4 products involved in secretion. J Biol Chem 264:12394–12401.

Zhang Y, Zhou L, Miller CA (1998) A splicing variant of a death domain protein that is regulated by a mitogen-activated kinase is a substrate for c-Jun N-terminal kinase in the human central nervous system. Proc Natl Acad Sci USA 95:2586–2591.